

ELIMINATION OF ASSEMBLY-INDUCED PACKAGE CRACKS IN PLASTIC SOIC

Jose Cesar de Guzman
Elmer Epistola
Analog Devices Phils., Inc.
South Expressway, Paranaque
Metro Manila, Philippines

and

Manolo G. Mena
Professor and Chairman
Department of Mining and Metallurgical Engineering
College of Engineering
University of the Philippines
Diliman, Quezon City, Philippines

ABSTRACT

Considerable amount of information and knowledge is available on moisture-induced package cracking, especially on surface mount devices. During IC assembly itself, plastic packages are subject to thermal and mechanical stresses which may lead to package cracking or degrade package strength, thus making the package more susceptible to moisture effects. This study was conducted to characterize and understand assembly-induced package cracking in SOIC's. Probable sources of thermal and mechanical stresses were identified by analyzing each station of the SOIC back-end assembly process. Each package cracking mechanism identified was defined in terms of its associated failure modes and rootcauses.

The critical areas identified include mechanical deflashing, dambar removal, lead forming, singulation and IR ink curing. Mathematical models of the cracking mechanisms in these areas were developed and used to understand process input variables that affect the tendency of a package to crack. Evaluations, simulations and failure history reviews were then done to verify and substantiate the models with actual data.

Process improvements were then defined based on the assembly input variables verified to be critical to SOIC package cracking tendency. These improvements include tooling modifications which reduces stresses during assembly, prevention and assignable causes through design and system improvements and tool life evaluations which eliminate potential sources of worn out tools. Package robustness measures such as anchor holes, improved tie-bar designs v-grooves and dimples were also analyzed. Process controls, monitors, contingency measures and short-looped reliability tests were likewise developed for early detection and containment package crack occurrences on the line.

Results of the study showed that assembly-induced package cracking may be minimized through proper management of mechanical and thermal stresses at back-end assembly. Key areas identified include:

- Reduction of mechanical stresses through process and tooling design improvements;

- Elimination of process deviations and/or problems by using effective process controls and early detection monitors; and
- Package robustness enhancement schemes.

1.0 INTRODUCTION

The semiconductor plastics packaging technology has evolved and advanced in so many aspects over the last two decades. Throughout these years the industry has had to contend with package cracking issues that had come and gone with each technological stride. Studies have shown that, indeed, package cracking mechanisms evolved with technology.

Early major plastic package cracking occurrences in plastic assembly most commonly involve 300 mil narrow PDIPs. The cracks were eventually traced to the large mechanical stresses of plate molding and single-stage forming. These phenomena have influenced the popular exodus from aperture plate molding to conventional molds and from single stage to multiple stage forming. However the switch did not assure that parts are completely safe from package cracking. Every now and then crack failures were being encountered and analyzed as being connected to various assembly related causes. These root causes vary from design, material/tooling conditions to human errors, etc. This is true not only in several but many other foundries which makes package cracking an industry-wide problem.

Semiconductor packages become more susceptible to cracking and delamination as they become thinner. With the continuous growth of SOIC assembly operations at ADPI, a better understanding of package cracking mechanisms has become imperative. This necessitates accurate failure analyses of all package crack occurrences.

Failure analysis of package cracks down to rootcause level is difficult. Oftentimes it can not be done by a single individual. A more viable approach is for a group of engineers from various disciplines of semiconductor assembly to analyze and address the problem.

Most of the findings presented in this study were generated through team approaches. The collective effort and knowledge of assembly, failure analysis, and reliability engineers ensured that even minute details of SOIC back-end assembly operations are considered in this study.

Evaluations and simulations to verify or disprove package cracking hypotheses were conducted by the team. The results of these evaluations and simulations were then complemented with findings from Scanning Electron Microscopy (SEM), X-ray radiography, fractography and other failure analysis techniques.

The end-product of all these activities is a compendium of well-characterized potential and actual package cracking mechanisms that may be encountered with SOIC's. Corrective actions to minimize package crack occurrences have likewise been identified and, in some cases, already instituted. Finally, the team has identified process controls and contingency measures for the early detection and containment of SOIC package cracks.

The pursuit of package crack-free assembly operations is a must in all packaging houses. The objective of this paper is to be the technical backbone for spearheading the realization of this goal.

In summary, this study was conducted to:

- 1) acquire a thorough understanding of why package cracks occur in SOICs;
- 2) institute process corrective actions, controls, and contingency measures to minimize, if not preclude package cracking in SOICs; and
- 3) lay down the foundation towards achieving package crack-free assembly operations at ADPI.

2. SOIC PACKAGE CRACK MECHANISMS

Potential cracking mechanisms for ADPI's SOIC package had been identified through process modelling and literature research. Process modelling identified package cracking mechanisms that are assignable to the assembly process, package design, and their interaction with each other. On the other hand, literature research identified mechanisms that arise out of imperfections in the package itself and are therefore not confined to the SOIC alone. Actual and simulated occurrences are presented whenever available and applicable to the package cracking mechanism being discussed. Each of the identified mechanism is characterized and discussed below.

2.1 Mechanical Overstress

As expected, package cracking is usually traceable to process anomalies that expose the package to mechanical overstress. In this study, each of the back-end assembly station was scrutinized for possible contributions to mechanical oversteering.

2.1.1 Cracks due to Mechanical Deflash

The excess plastic materials that protrude from the top-bottom interface of the package after molding are known as flashes. These flashes are sheared off the interface using a deflash blade during mechanical deflashing.

A small deviation from the intended direction or position of the deflash blade may result in the package being hit by the blade. Deviations in the package outline of a package can also make it more prone to cracks caused by mechanical-deflashing.

Package mismatch is defined as excessive lateral or vertical displacement of the bottom package with respect to the top package. Package offset is defined as excessive lateral or vertical displacement of the package center with respect to the leadframe center.

A unit with an unacceptable amount of package mismatch will have the bottom package protruding beyond its top package on one side.

The mechanical stress exerted by a deflash blade hitting on the bottom package increases as the package mismatch increases. The side where the bottom package protrudes may be modelled as a cantilever beam loaded by the deflashing force F . This force F produces a reactive force S_n at the top and bottom package interface. This model is shown in Fig. 2.1.1a.

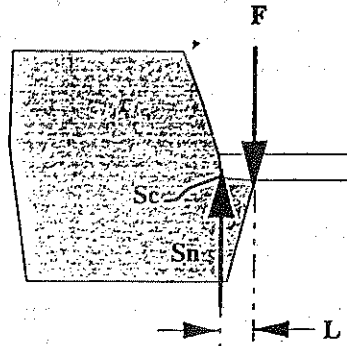


Figure 2.1.1a. Model of a package with excessive mismatch subjected to the deflashing force

The over-all stress S_c created at the top and bottom package interface is given by the product of S_n and a geometric stress concentration factor SCF. The stress concentration factor is due to the corner produced by the top and bottom package interface^[3] and is given as:

$$SCF = 1 + 2 (c/a)^{1/2}$$

where

$2c$ = cracklength and
 a = radius of curvature of the corner

Thus,

$$S_c = S_n (1 + 2(c/a)^{1/2}) \quad (1)$$

or

$$S_c = S_n (1 + 2(L/2a)^{1/2})$$

since L is the cracklength based on the assumption of the model that the crack is the imaginary cavity formed by the top and bottom packages.

S_c must exceed the fracture strength σ_F of the package for the stress to result in cracks. The parameter σ_F ^[3] measures the strength of a material in the presence of cracks^[3] and is given

as:

$$\sigma_F = (m K_{Ic}) / ((\pi L/2)^{1/2}) \quad (2)$$

where

K_{Ic} = fracture toughness
 and
 m = the cracks's geometric stress concentration factor
 = $1 + 2 (L/(2a))^{1/2}$

Equation (1) shows that the stress experienced by the package's parting line may be reduced by maximizing the allowable radius of curvature of the chamfer on both sides of the package.

Package cracking due to the bottom package being hit by the deflash blade because of excessive package mismatch was simulated in 60 mil SOIC packages.

Microfocus Xray radiography and SEM analysis showed that units with package cracks exhibited greater package mismatches than those with no package cracks, as shown in Table 2 below.

Table 2. Package Mismatches of the Simulated 60 mil SOIC packages.

With Cracks	Without Cracks
52.3 um	-10.4 um
50.2 um	0.0 um
33.6 um	5.2 um
45.1 um	-8.4 um
	4.2 um
	-15.7 um
	4.2 um
	0.0 um
	-6.3 um
	0.0 um

Package mismatch in units with cracks averaged 45.3 microns with a standard deviation of 8.3 microns. On the other hand, package mismatch in those with no cracks had an average and a standard deviation of only -2.718 microns and 7.099 microns, respectively.

A negative value for the mismatch means that the top package is protruding beyond the bottom package at the unchamfered side. The data above supports the discussion earlier that cracking occurs when there is excessive protrusion of the bottom package beyond the top package at the unchamfered side. The absence of package cracks at the chamfered side of units with

negative values of mismatch also gives credence to equation (1) which predicts less stresses at the chamfered side of the unit.

Cracks produced by the deflash blade hitting the bottom package due to excessive mismatch are barely visible right after assembly. However, subjecting a unit with such cracks to thermal stresses like temperature cycling and IR reflow would result in larger cracks that propagate along the interface of the top and bottom packages, extending from one end of the unit to the other. Delaminations usually occur between the leads and the bottom package. Furthermore, cracks from this mechanism tend to propagate downwards at the ends of the package, usually terminating at or near the tiebars. A typical package crack of this nature is shown in Figure 2.1.1b.



Figure 2.1.1b Photo of an 8L SOIC package cracked by the deflash blade due to excessive package mismatch

The downward propagation of the crack at the ends of the package was traced to the internal delamination of the package from the die paddle and tiebars of the leadframe. The crack propagation simply followed the directions of these internal delaminations, supporting earlier observations that package cracks and delaminations interact significantly in thin packages like the SOIC.

A large package offset means that the leadframe may be centered and properly positioned with respect to the deflash blade, but the plastic body is not. This results in a greater exposure of one side of the package to the deflash blade. This greater exposure increases the chances of a package being cracked by the deflash blade.

Another factor affecting package crack mechanisms due to mechanical deflash is the adequacy of package nesting during this process. The adequacy of deflash die package nesting is quantified in terms of the seated area at the bottom of the package during deflashing. An inadequate package nest support results in greater flexural stresses on the package during deflashing. Package cracking occurs if the flexural stress exerted on the package exceeds the flexural strength of the molding compound.

Consider the package nest model shown in Figure 2.1.1c. Any force F acting on a point on the package where there is no nesting support underneath would produce a maximum bending

moment M at the edge of the package nest given by:

$$M = Fx$$

where x is the unsupported distance from the edge of the package to the edge of the nest.

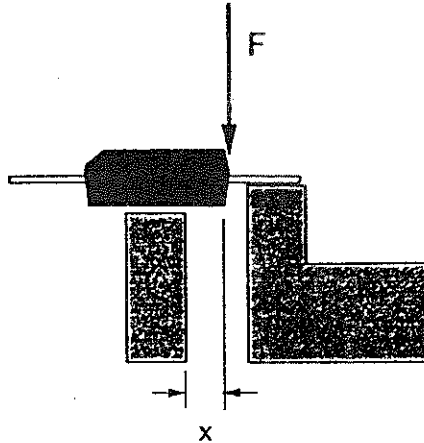


Figure 2.1.1c A model of the package nesting configuration of the deflash die.

The relationship between the bending moment and the bending stresses at a cross-section of the beam ^[2] in the model is given by:

$$\sigma = My/I \quad (3)$$

or

$$\sigma = (Fx)y/I$$

The flexural stress σ and bending moment M decrease as the moment arm x decreases.

Thus, equation (3) shows that the flexural stresses acting on the package during deflashing may be minimized by providing full nesting support at the bottom of the package.

An actual occurrence of package cracking and chipping due to inadequate nesting support was encountered in 1994 when ADPI was evaluating a new tool. The observed cracks tend to terminate at the edge of the package nesting, as shown in Figure 2.1.1d. This supports the earlier analysis that the edge of the package nest acts as a fulcrum for bending moments during deflashing, subjecting the package to flexural stresses that may cause package cracking. The said tool was returned to the vendor for modification to account for this effect.

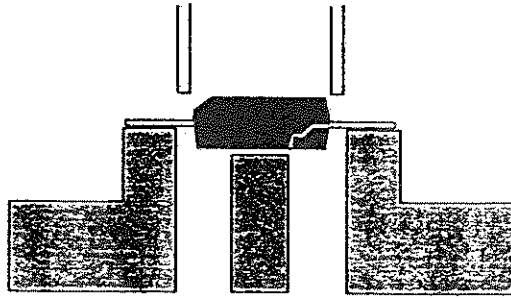


Figure 2.1.1d. Crack termination at the edge' of an inadequate package nest

2.1.2 Cracks due to Dambar Removal and Lead Trimming

The dambars connecting the leads to each other are punched out before the leads are cut from the leadframe. Although only the dambars and leads are subjected directly to the large mechanical stresses of the punch during dambar removal and lead trimming, a portion of these stresses are transmitted to the package. The mechanism by which stresses at the dambars and leads result in package cracks also occurs during lead forming. This mechanism is described in more detail in the next section.

2.1.3 Cracks due to Lead Forming

The leads are subjected to large mechanical stresses during leadforming but only a portion of these stresses are transmitted to the package because the leads are clamped during the process. However, if the axial component of the lead forming stress exceeds the sum of the clamping stress and the lead-to-package adhesion strength, the leads may be pulled out of the package. Lead pulling is frequently accompanied by package cracking.

The axial component σ_x of the forming stress on each lead is simply the axial component F_x of the forming force divided by the cross-sectional area A of the lead.

Consider the leadforming model in Figure 2.1.3a. When the lead is not yet bent, the forming force F acts perpendicularly on the lead, with only shearing stresses acting on any cross-section of the lead that's perpendicular to the lead's axis. Under such circumstances, no lead pulling effect is taking place.

As the lead is bent, any cross-section perpendicular to the lead's axis is subjected to an increasing normal or axial stress σ_x . These normal stresses act parallel to the lead's axis and tend to pull on the lead itself.

Based on Figure 2.1.3a, the relationship between the forming force F and the axial stress σ_x it produces is given by:

$$\sigma_x = F \sin \theta / A \quad (4)$$

$$\text{since } F_x = F \sin \theta.$$

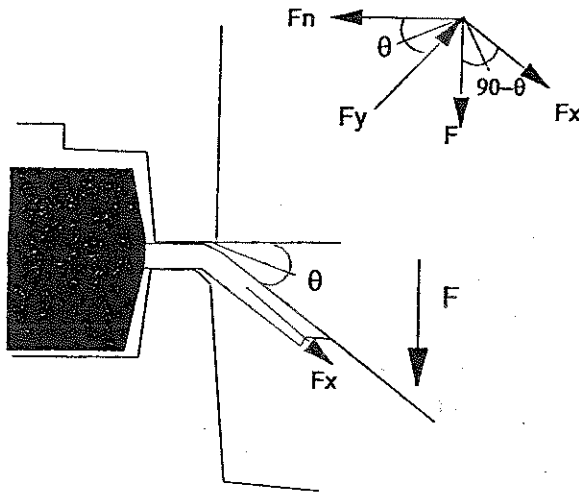


Figure 2.1.3a. Model of a lead acted upon by the leadforming force.

Thus, the axial stress σ_x increases as the forming angle increases. This also means that the lead pulling effect increases as the forming angle increases.

The total clamping stress S_{CL} on a lead is given by:

$$S_{CL} = F_{CLTOP}/A_{TOP} + F_{CLBOT}/A_{BOT}$$

where F_{CLTOP} and F_{CLBOT} are the clamping forces on the top and bottom surfaces of the lead, respectively, while A_{TOP} and A_{BOT} are the areas on the leads where the clamping forces are applied.

Lead pulling and package cracking occurs if the axial stress σ_x exceeds the sum of the clamping stress and the effective adhesion strength of the lead to the package, or

$$\sigma_x > S_{CL} + S_{ADHESION} \quad (5)$$

where $S_{ADHESION}$ is the adhesion strength of the lead to the molding compound.

The lead clamping stress has a maximum value beyond which the leads would already be deformed or damaged by the clamp. Thus, in Equation (5), only $S_{ADHESION}$ may be improved upon to prevent lead pulling during forming. The lead-to-package adhesion strength may be improved by increasing the contact area between the lead and the molding compound. Anchor holes of well-chosen shape and size may also be placed on the contact area to prevent lead pulling.

Equation (4) shows that mechanical stresses during forming may be minimized by using smaller forming angles for each forming stroke. However, this may necessitate an increase in the number of strokes for forming the leads.

Another source of mechanical overstress during leadforming is the form stripper, which holds down the leads during forming. Dimensional and set-up problems can result in the package being hit by the form stripper itself.

When the form stripper hits the top surface of the package, no damage may be induced, on this part of the package. However, the form anvil pushes the leads up as soon as the stripper hits the package. These lead deflections result in mechanical overstresses at the lead-package interface. If the stresses exceed the flexural strength of the molding compound at the affected areas, package cracking will occur. To model this mechanism, each lead may be considered as a cantilever beam of uniform cross-section loaded by a concentrated force F at the point where the form anvil touches the lead. The reactions of the system to this force F consists of an equal but oppositely directed force F_R and a moment at the lead-package interface. Figure 2.1.3b shows a graphical representation of this model.

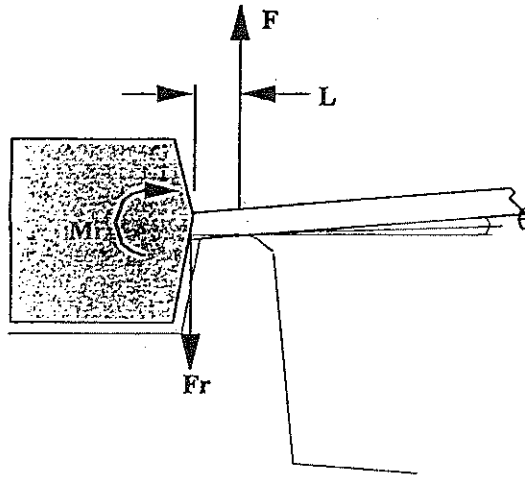


Figure 2.1.3b. Model of a lead deflected by the form anvil during singulation.

Elastic deflection mechanics established the relationship between F_R and the amount of deflection of the beam under such conditions ^[2] as:

$$F_R = (3\delta EI) / (L^3) \quad (6)$$

where

- F_R = the force at the lead-package interface;
- δ = maximum lead deflection;
- L = the lead's effective cantilever length;
- E = the LF's modulus of elasticity; and
- I = the lead's moment of inertia.

Given the flexural strength F_s of the molding compound, the maximum angular deflection θ_{crit} of the leads before package cracking occurs may be estimated as

$$\theta_{\text{CRIT}} = \arctan (\delta/L)$$

for $F_s = F_R/A$ where A is the bonding finger area.

Thus, package cracks at the lead-package interfaces would result if the leads are bent by the form anvil by an angle greater than θ_{CRIT} when the form stripper hits the package.

Form strippers are normally designed to conform to the package outline. Form stripper inversion during set-up can cause the package cracking mechanism described above. If the form stripper is inverted during singulation, the unchamfered side of the top package would be hit directly by the stripper. This situation is depicted in Figure 2.1.3c.

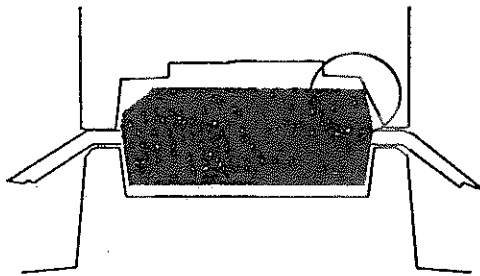


Figure 2.1.3c Package cracking due to form stripper inversion

Package cracks caused by this mechanism are found at the interface of the top and bottom packages, traversing under the leads. This is expected since the mechanical overstresses resulting from the lead deflections produced by this mechanism occur at the interfaces of the leads and the bottom package. This mechanism is also characterized by bent leads.

2.1.4 Cracks due to Singulation

Singulation is the back-end assembly process wherein the units are separated from each other. This is done by allowing a stationary singulation die to shear off the tiebars at the ends of the package as the package is pressed downwards.

Package cracking may occur during singulation if the singulating die has worn out and requires a larger force to shear off the tiebars. The cantilever beam model described by equation (6) can again be used to characterize the relationship between the singulating force and the tie bar deflection^[2] during singulation.

Thus,

$$\sigma = (3\delta EI) / (AL^3) \quad (7)$$

where

σ = the stress at the tiebar-package interface;
 δ = the maximum tiebar deflection;
 L = the tiebar's effective cantilever length;
 E = the LF's modulus of elasticity;
 I = the tiebar's moment of inertia; and
 A = the lower tiebar-package interface area.

The above model again supports observations on the line that large tiebar deflections during singulation due to a worn-out die results in delaminations between the tiebar and the lower package. Worse cases also result in package cracks.

Another aggravating factor for package cracking during singulation is the mechanical resistance of the mold gate flash to the singulating die. The mold gate flash is the excess plastic material at the mold gate area of the package. Again, a mold gate flash acts like a cantilever beam sticking out of the package's end. Thus, the stress acting at the mold gate area of the package assuming that it has enough protrusion to be hit by the singulating die may also be modelled using equation (7) above. The additional stress resulting from this mechanism may interact with stresses induced by other factors such that package cracking tendency is aggravated.

2.2 Thermal Overstress

Thermal overstress produces mechanical stresses that may result in package cracks. Cracking mechanisms that are caused or triggered by exposure of the package to excessive temperatures are explored below.

2.2.1 Cracks due to Differences in Coefficients of Thermal Expansion

Differences in the coefficients of thermal expansion of the piece parts used to assemble the package produce internal mechanical stresses. These stresses arise because of differences in thermal expansion among the pieceparts, creating tensile and compressive forces within the package. Minimizing thermal expansion mismatches among the components of a package would reduce the occurrence of package cracks from thermomechanical stresses.

Minimization of the mismatches in the thermal expansions of the individual parts of the package may be done through careful selection of the components. The dimensions, morphologies, and coefficients of thermal expansion of these components must be chosen such that the package is subjected to low internal mechanical stresses when thermal stressing is applied.

Consider two different materials A and B that were fused together at a high temperature T_H . After cooldown to ambient temperature T_{AMB} , both materials A and B should have contracted by $L\alpha_A(T_H - T_{AMB})$ and $L\alpha_B(T_H - T_{AMB})$, respectively, where L is the length of the two-material system and α is the coefficient of thermal expansion (CTE) corresponding to the material.

However, since materials A and B are fused to each other, they were both forced to contract by the same amount δ . The material with a lower α would then be under compression while the material with a higher α would be under tension.

The stress σ_{INT} resulting in each material ⁽⁴⁾ may be expressed as:

$$\begin{aligned} \sigma_{INTi} &= \varepsilon_i E_i \text{ OR} \\ \sigma_{INTi} &= ([\delta - L\alpha_i (T_H - T_{AMB})] / L) E_i \end{aligned} \quad (8)$$

where ε_i is the strain undergone by the material and E_i is the modulus of elasticity of the material.

Delamination and/or package cracking occurs if these internal stresses exceed their corresponding adhesion or fracture strength in a part of the package. Equation (8) above shows that the internal stress produced increases as the difference between the actual and unconstrained strains increases. A larger modulus of elasticity also results in a larger stress for a given strain.

Thus, internal stresses within an IC package may be minimized by choosing components whose thermomechanical characteristics will result in matched thermal expansions.

Some of these characteristics are shown in Table 4.

Table 4. Material Properties Affecting Package Cracks due to Thermomechanical Stresses

Material	Thermal Coeff of Expansion (ppm/degC)	Thermal Conductivity (W/m C)	Young's Modulus (GPa)
Molding Compound	21	0.6	18
Copper Leadframe	17	398	119
Alloy 42 Leadframe	5	15	145
Silicon Die	3	157	131

Unfortunately, matching the thermomechanical properties of the components of a plastic package is not easy since there is a large difference between the CTEs of the molding compound and the Silicon die. This means that reducing the tendency of a package to delaminate or crack

may result in a higher tendency for the die crack. The emergence of sophisticated finite element analysis software packages lately has helped in surmounting these difficulties though.

2.2.2 Cracks due to Thermal Degradation of the Package

The molding compound degrades at excessively high temperatures due to the volatilization of the side radicals in the molecular structure of the molding compound. This degradation is manifested as an irreversible increase in the brittleness and decrease in the fracture strength of the material.

IR cure is a back-end assembly step for curing the ink marks on the package. It consists of exposing the marks to infrared rays for a predefined period of time. Since the time of IR exposure for every cure cycle is constant, IR overcure can happen only if the package is subjected to multiple IR cure cycles or jamming in the brander occurs.

Simulations were conducted by Plastic EOL Engineering to verify the package cracking mechanism discussed above. The results of the simulations showed that an exposure equivalent to six (6) IR cure cycles are needed to make the package susceptible to cracking even at normal levels of mechanical stressing.

Aside from ink mark and package discoloration, packages that underwent thermal degradation due to IR overcure are also characterized by topographical irregularities and, in extreme cases, blisters on the package surface.

Since the surface of the package that was directly exposed to the IR rays underwent the worst thermal degradation, its fracture strength would also be significantly lower than the other surfaces of the package. This explains why cracks in overcured packages tend to propagate towards the degraded surface of the package, a phenomenon that was observed consistently in the package cracking mechanism described above. Figure 2.2.2 below shows a photograph of a typical package crack caused by IR overcuring.

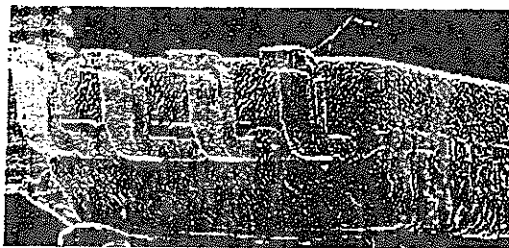


Figure 2.2.2 Cracked package due to IR Cure

2.2.3 Cracks due to Moisture Ingression

Moisture ingress into thin plastic packages can likewise lead to package cracking upon

exposure of the packages to excessively high temperatures. The trapped moisture inside a package is forced to escape when sudden heating of the package occurs, creating large stresses due to internal vapor pressure build-up. Package cracking and delamination result if these stresses exceed the fracture strength of the package.

Fukuzawa, et. al., had shown that the maximum stress $\sigma_{MAX}^{[5]}$ experienced by a package when it is suddenly exposed to high temperatures is given by:

$$\sigma_{MAX} = 6K(a/t)^2P \quad (9)$$

where

K = geometric factor (=0.05 for a square die);
 a = die paddle length;
 t = thickness of the plastic under the paddle; and
 P = internal vapor pressure, which is a function of the temperature and the amount of moisture inside.

In this equation, the maximum bending stress occurs at the center of the length of the die paddle. Cracking occurs when σ_{MAX} exceeds the critical stress σ_c , which is a function of the strength of the molding compound at the critical temperature.

This mechanism is widely known in the semiconductor industry where it is also commonly referred to as "popcorn cracking."

Equation (9) above shows that thinner packages are more susceptible to popcorn cracking.

As such, the SOIC is highly vulnerable to this package cracking mechanism. Equation (a) however appears not to apply to TSOP's where moisture can easily diffuse through the very thin layer of plastic.

2.3 Stress Concentrators

2.3.1 Voids

Voids in the plastic package of a unit act as stress concentrators. Equation (10) may be used to model a void as a stress concentrator. Thus,

$$S_c = S_n (1 + 2(c/a)^{1/2}) \quad (10)$$

where

2c = cracklength and
 a = radius of curvature of the corner.

Based on the graphical representation of this model in Figure 2.3.1a, the radius r and diameter d of the void are the radius of curvature and cracklength, respectively, in the equation.

Thus,

$$S_c = S_n(1 + 2(d/2r)^{1/2}) \quad (11)$$

or

$$S_c = 3S_n.$$

Thus, a void tends to multiply stresses acting on it by a factor of 3.

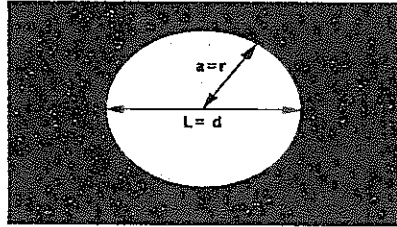


Figure 2.3.1a. Graphical representation of a void as a stress concentrator.

2.3.2 Burrs and Microcracks

Burrs on the leadframe and microcracks in the package also act as stress concentrators. Equation (10) above may also be used to model a burr or a microcrack as a stress concentrator.

Again,

$$S_c = S_n(1 + 2(c/a)^{1/2})$$

where

$2c$ = cracklength and

a = radius of curvature of the corner.

However, the radius of curvature is much smaller than the cracklength in burrs and microcracks. Thus, burrs and microcracks act as worse stress concentrators than voids.

3. SOLUTIONS TO PACKAGE CRACKING

A master plan to address package cracking issues may be developed based on the practical implications of the mathematical models used to characterize the package cracking mechanisms discussed earlier. Table 3a shows these mechanisms and their respective modelling equations.

Table 3a. Package Cracking Mechanisms and their Modelling Equations

CRACKING MECHANISM	MODELLING EQUATION
Deflash blade hitting the package	$S_c = S_n(1 + 2\sqrt{L}/(2a))$ (1)
Inadequate package nesting	$\sigma = (F_x)y/l$. (3)
Leadforming Overstress	$\sigma_x = F \sin \theta/A$ (4)
Form Stripper Inversion	$F_R = (3\delta EI)/(L^3)$ (6)
TCE Incompatibilities	$\sigma_{INTI} = ([\delta - L\alpha_i(T_H - T_{AMB})]/L)E_i$ (8)
Popcorn Cracking	$\sigma_{MAX} = 6K (a/t)^2P$ (9)
Presence of Stress Concentrators	$S_c = S_n (1 + 2 \sqrt{c/a})$ (10)

Package cracking may occur if the part is subjected to excessive thermal and mechanical stresses. As such, the stresses to which the parts are subjected to during assembly must be managed appropriately.

In this study, three areas of approach were identified to manage these stresses on the line.

These are:

- 1) enhancement of package robustness through internal package design improvements;
- 2) minimization of stresses inherently present in the process; and
- 3) elimination of stresses due to assignable deviations in the process.

3.1 Package Robustness Enhancement

Resistance to thermo-mechanical stresses may be improved through careful internal package redesign. The modification intent is to help the package components be more firm and stable when subjected to various assembly induced external stresses.

3.3.1 Lead anchoring

The leads are subjected directly to mechanical stresses during debar, lead cut and forming. A portion of the stress is transmitted by the leads to the package, as discussed in section 2.1.3. Provision of anchor holes between the leadfinger and the package outline increases the flexural and adhesive strengths of the plastic material surrounding the leads. This prevents the leads from being pulled from the package due to the stresses transmitted through the leads during debar, lead cut, and forming. This is illustrated below.

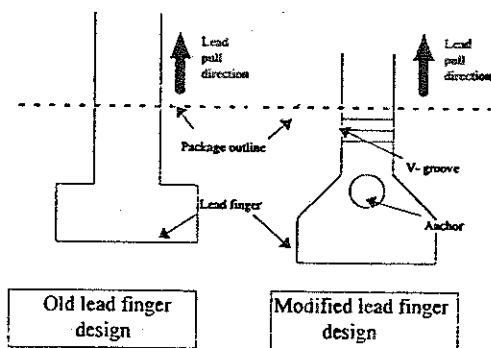


Figure 3.1.1 Anchor holes in the bonding fingers prevent lead pulling

Table 3.1.1 shows lead pull test data for leadframes with and without anchor holes. The leads with anchor holes need a force of about 1900g to pull as compared to the 950g needed for leads on leadframes without anchor holes. The usual mode of test result of leadframe with anchor hole is broken leads, which means the plastic package remained intact while the copper lead finger breaks. On the other hand the mode of test result for the leadframe design without anchor hole is usually pulled out lead. This means that the copper lead finger did not break but was completely pulled out from the package.

Table 3.1.1a. Lead pull Test Results (Kg)

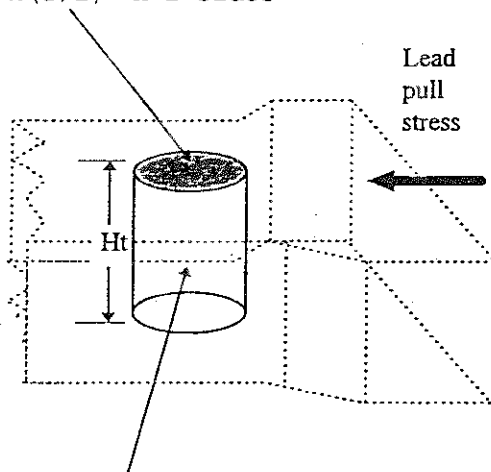
Pad size	S/S	Avg	Std	min	max	mode
w/AH 95x130	20	1.92	0.108	1.7	2.1	100% Broken
95x150	20	1.83	0.137	1.6	2.1	100% Broken
w/o AH 88x150	24	.95	0.28	0.25	1.5	90% Pulled

3.1.2 Leadframe to package ratio

The adhesion strength of the molding compound to the copper leadframe depends on the area of contact between these two materials. Putting an anchor hole on the lead finger increases this contact area by an amount equal to the inner surface area of the cylindrical hole but decreases

it by an amount equal to twice the area of the corresponding circular hole. This is illustrated in Figure 3.1.2a.

$$A_c = \text{Lost surface area due to hole} \\ = \pi(D/2)^2 \times 2 \text{ sides}$$



$$A_{cy} = \text{gained surface area of anchor hole} \\ = (\pi D Ht)$$

Ht = Leadframe thickness

Figure 3.1.2a. Plastic-Copper contact areas gained and lost with the introduction of anchor holes

As the hole size increases, the effective surface area associated with the adhesive and flexural strengths of the compound also increase. However, an increase in the size of the lead anchor holes decrease the tensile strength of the leads. Table 3.1.2 shows the physical properties of the molding compound and leadframe used in a typical SOIC assembly. The interactions between the material strengths of the leadframe and plastic compound were computed based on this table and plotted as shown on Figure 3.1.2b.

Table 3.1.2 Physical Properties of Typical SOIC Molding Compound and Leadframe

Material: Epoxy Novolac Molding Compound.

Flexural Strength = 12 Kg/mm²

Adhesive Strength = 104 Kg/cm²
= 1.4kg/mm²

Leadframe: Copper, 1/2 Hard annealed.

Tensile Strength = 40.78 Kg/mm²

Anchor diameter vs Material Strength Interactions

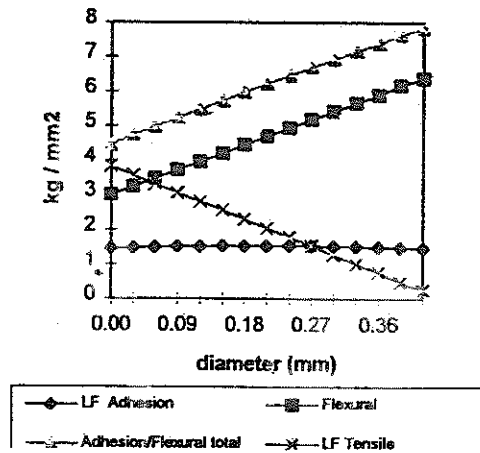


Figure 3.1.2b Relationship between anchor hole diameter and material strength

The adhesion strength does not increase linearly with the anchor hole diameter. Equation (12) below gives the relationship between the adhesion strength (AS) and the size of the anchor holes introduced.

$$AS = ((LFS - A_c) \times 2 \text{ sides} + A_{cy}) \times K \quad (12)$$

or

$$AS = ((LFS - pD^2/4) \times \text{sides} + pD \text{ Ht}) \times K$$

where:

- AS = Overall adhesion strength.
- LFS = Lead finger surface area inside the package outline.
- K = Adhesion strength of the 6300H molding compound with Cu leadframes. = 1.04 kg/mm²
- A_c = Circular area lost due to the anchor hole
- A_{cy} = Cylindrical surface area of the anchor hole.
- D = Diameter of the anchor hole
- Ht = Thickness of the leadframe (.2108 mm)

Maximum adhesion strength may be obtained by equating the first derivative of equation (12) to 0. Thus,

$$\frac{dAS}{dD} = ((-2pD/2) + p \text{ Ht}) K = 0$$

or

$$Ht = D. \quad (13)$$

Equation (13) above shows that maximum adhesion strength is obtained by using anchor holes whose diameters are equal to the thickness of the leadframe.

The graph shown in Figure 3.1.2c depicts that at approximately 8.0% anchor hole to leadfinger surface area ratio, the adhesion strength is maximum at 1.533 kg/mm² where the diameter is approximately equal to the thickness. The most significant improvement at this ratio is flexural / adhesion combined strength which is at 6.23 kg/mm². This is an improvement of 1.75 kg/mm² from a leadfinger without anchor hole at 4.46 kg/mm².

% Anchor hole area vs Pkg to LF Adhesion strength

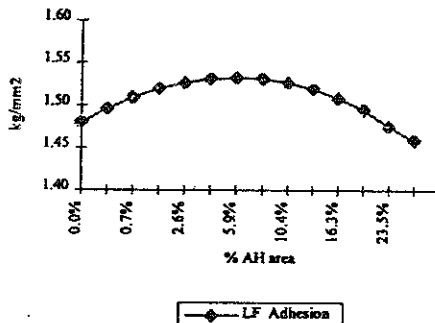


Figure 3.1.2c. Relationship between % anchor hole area and adhesion strength

3.1.3 Pad Depression

The amount of depression of the pad should take into account package dimension and die thickness. The pad depression must accommodate the die in a position wherein the centers of gravity of the die and the package coincides with each other. This promotes a well-balanced absorption of stresses within the package and therefore results in a more robust structure.

3.1.4 Tie Bar Design

The tie bar is subjected to mechanical stresses during singulation. However, unlike the leadfinger, it is intended to be sheared off from the package. The tie bar must be firm enough to hold the package during assembly until final forming but must also be frail enough to be knocked out during singulation without affecting the plastic material in contact with it.

Figures 3.1.4a and 3.1.4b show the evolution of the tie bar design for the 8 lead SOIC.

Earlier there was only a single tie bar link between the rail and the die pad. This tie bar link has a width of .008" (.2032mm.), which translates to a tensile strength of 1.74kg/mm², compared to the 0.25 kg/mm² flexural strength of the adjacent plastic material.

This evolved with the introduction of the tie bar and die pad anchor holes which divided the link into two. This modification made the tie bar lighter for shearing force with an individual 1.31 kg/mm^2 tensile strength. Its ability to support the pad and package likewise improved with a total tensile stress of 2.62 kg/mm^2 . The plastic material also benefitted with an additional flexural strength of 1.28 kg/mm^2 at the anchor holes.

A recommended approach to further improve package robustness at the package ends is by coupling the tie bar and die pad anchor holes. This will further increase flexural strengths with a bigger anchor hole and this will enhance its resistivity to moisture ingress.

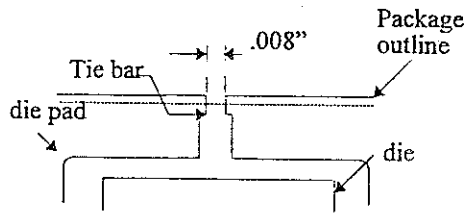


Figure 3.1.4a Evolution of the tie bar design (Revision a)

Revision (b) :

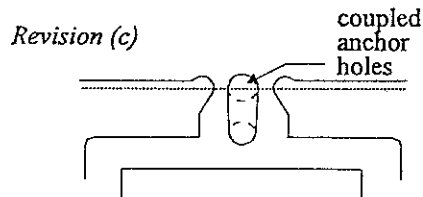
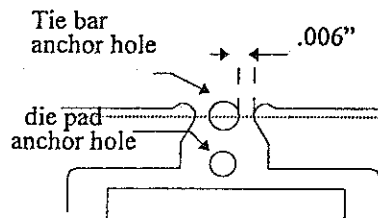


Figure 3.1.4b. Evolution of the tie bar design (Rev b & c)

3.1.5 V-Groove

The V-groove increases the effective length of the leads or tie bars, deterring moisture ingress and improving the adhesion between the leadframe and the package. (see Figure 3.1.5)

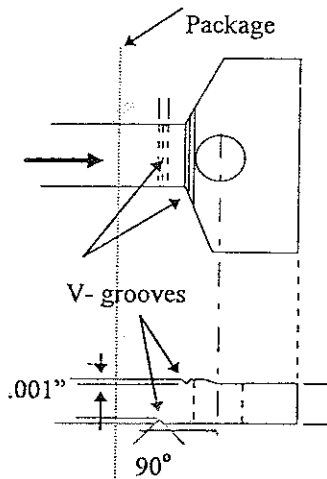


Figure 3.1.5 V-Grooves on the leadframe

3.1.6 Dimples

The dimples are balanced indentations on the die pad backside surface. The impressions serve as tiny stress absorbers specially when the package is suddenly exposed to high temperatures. Equation (9) in Table 3a shows that the stress due to the internal vapor pressure build up when package is subjected to heat is directly proportional to the die pad length (a). Provision of dimples decreases the effective length to δ , the spacing between the dimples. This drastically reduces the internal stress in the package during soldering.

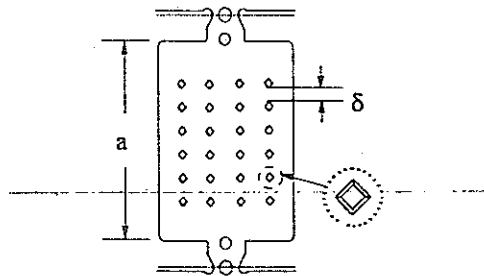


Figure 3.1.6 Dimples on the die paddle

3.2 Minimal Stress during DTFS

The package needs maximized support at the leads and package and minimized impact due to various stresses induced on the leads from junk to singulation.

3.2.1 Deflash die lead support

The deflash die must support the leads similar to the way the dambar die supports the leads during the debar operation. This lessens the debar/debar blade's impact on the package. (See fig. 3.2, Revision d).

3.2.2 Deflash die package support

The deflash die must support the entire width and length of the package to prevent it from tilting and hitting the edge of the anvil as discussed in section 2.1.1 (See Figure 3.3, Revisions b to d).

Modifications of the Deflash/Debar die design

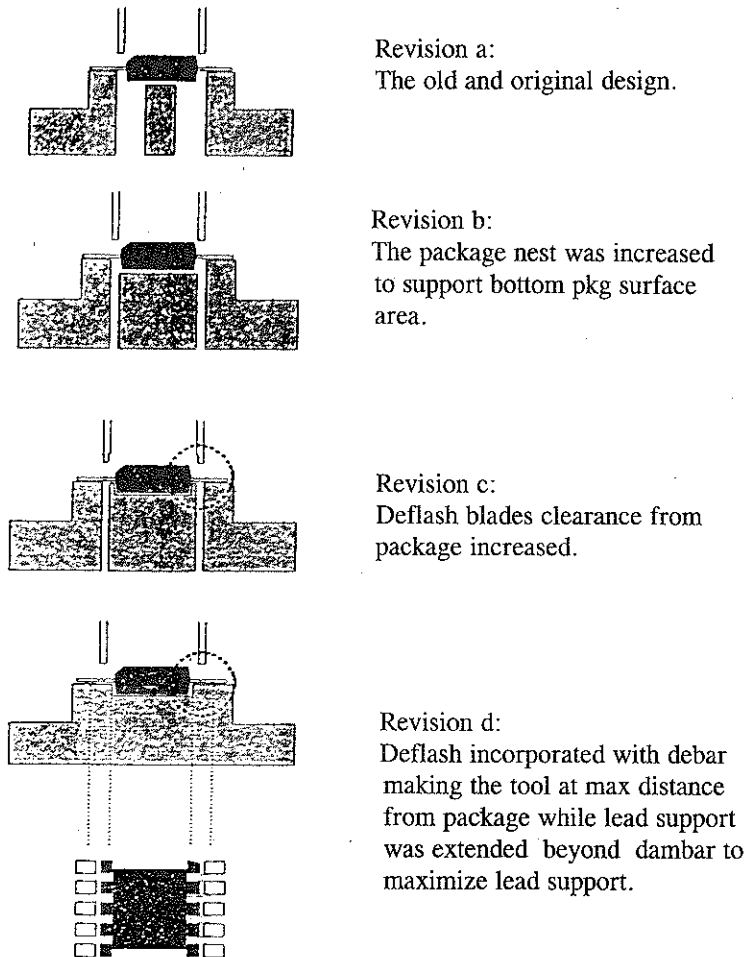


Figure 3.2.3 - Deflash/Debar modifications

3.2.3 Deflash blade proximity to the package

The proximity of the deflash blade to the package is critical, especially when there is a mismatch between the top and bottom packages, as discussed in section 3.1.1). Several modifications were made to address this concern until the deflash was incorporated with the debar operation making the punch at farthest distance from the package but leaving the sideflash at an acceptable level at .008" (see Figure 3.2.3).

3.2.3 Form stripper and anvil

The stripper must maximize its clamping on the leads close to the area covered by the anvil at the opposite side. This is to keep the lead shoulder secure and intact during forming, which applies a bending force directly on the leads itself. (See Figure 3.2.3)

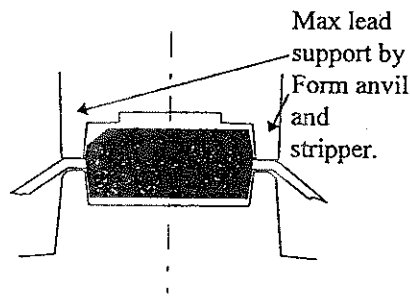


Fig. 3.2.3 Form Anvil and Stripper support

3.3 Assignable stress prevention

Package cracking is minimized if the package is not subjected to excessive or unnecessary mechanical stresses. Potential sources of problems leading to package cracks can be identified and avoided through tool and process improvements.

3.3.1 Strippers and ejectors spring tension lock

Previous designs of toolings allow adjustment of the spring tension through set screws. Adjustments only add unnecessary variables to the process. A preferred practice provides locking of the set screws requiring spring replacement when the spring has worn out. This is shown in Figure 3.3.1.

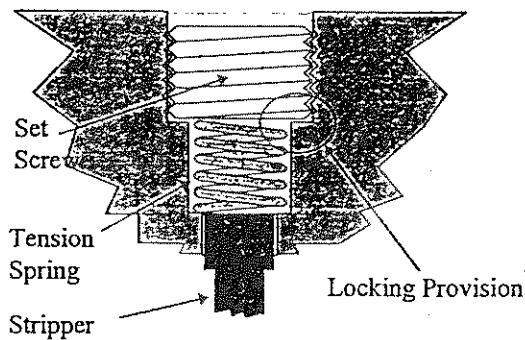


Figure 3.3.1 Locking of set screws to prevent adjustments

3.3.2 Fool-proof Misorientation-free Inserts

Inserts such as form strippers have the tendency to be installed in a reversed orientation, causing it to have unwanted contact with the package or leads that may eventually lead to a package crack or chip-out. Strippers and other inserts must be designed such that they would not fit in if misoriented during mounting. Another approach is to design them in a reversible fashion which allows mounting in any direction without any adverse effect on the IC package.

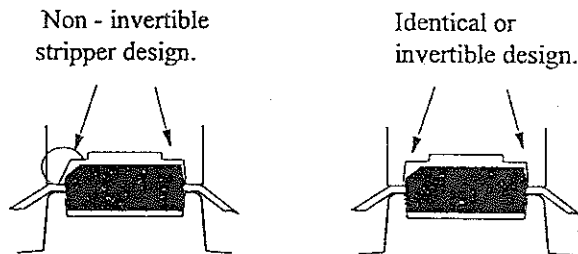


Fig. 3.3.2. Non-invertible an invertible form strippers

3.3.3 Prevention of debris accumulation:

Prevention of the accumulation of debris in toolings is important. Debris accumulation in toolings leads to sensor errors, jamming, and even package cracking. The accumulation of debris in toolings may be prevented by:

- a) provision of relief angles for the deflash/debar holes;
- b) provision of blow-offs and vacuum directed towards every anvil, i.e.; dejunk, debar, lead, cut, forming and singulation;

- c) provision of sensors for all blow-off and vacuum stations that trigger an error when jamming or clogging is sensed; and
- d) provision of enough clearance between package and clamping blocks/dies. The clearance provides space for debris that eluded blow off and vacuum and allows the debris to be blown on/off at the next stroke.

3.3.4 Tool life evaluation

The most effective way of preventing package cracks due to worn out parts is to replace them before they become worn out and cause undue stress on packages. Part of an ongoing tool life evaluation at ADPI identified tools and inserts which directly influence cracking in packages if they reach the worn out stage. Table 3.3.4 enumerates the critical toolings with corresponding response attributes and their direct effects on the package.

Table 3.3.4 Critical Toolings and their Attributes

Critical Area	Response	Effect on package
Punches: Lead Cut	Uncut Lead	Pulled lead
Strippers: Debar Lead cut Form	Crevice Uncut lead Lead bow	Crack Pulled lead Pulled lead
Dies: Lead cut Form Singulation	Uncut lead Lead bow Chip out	Pulled lead Pulled lead Pulled tie bar
Spring Tension: Form stripper Form ejector	Lead bow Tool mark	Pulled lead Die crack
Form stripper Form ejector	Premature singulation	Delam/Crack
Singulation lifter	Bent leads Chip out	Pulled lead Delam/Crack

4.0 EARLY DETECTION AND CONTROL

Line monitors exist on the line to ensure that the process is within its control limits. Package robustness tests had been developed to complement these monitors for early detection of

package crack occurrences. These test must be part of real time and short loop monitors to ensure that all improvements and preventive measures are working. A contingency plan to handle package crack occurrences due to assignable causes was likewise formulated.

4.1 Early Detection Tests

ADPI's Reliability Engineering designed a package robustness test procedure that could provide results within a span of one day. Immediate test results are significant for early detection and resolution of any package crack occurrence.

An early detection test was developed by ADPI's Reliability Engineering. Dubbed as the "t=0" test, it involves moisture preconditioning via PCT prior to solder shock.

An experiment was done to confirm effectiveness of the PCT preconditioning of the "t=0" test. Samples were taken from a known mechanically stressed parts and a known good lot. The samples were divided into 16 groups of 25 and subjected to the "t=0" test procedure. Each sample was then inspected under 30x magnification for any trace of crack. Table 4.1b below shows the results of the experiment.

Table 4.1b "t=0" Package Crack Inspection Results

Solder shock	Mechanically stressed parts		Good units	
	w/precon	w/o precon	w/precon	w/o precon
1x	1/25	0/25	0/25	0/25
2x	1/25	0/25	0/25	0/25
4x	1/25	0/25	0/25	0/25
8x	1/25	0/25	0/25	0/25

Based on the results, the PCT preconditioning is effective in inducing early life failures. Thus, the "t=0" test may be used to accelerate potential package crack failures. The number of early life failures due to cracked packages did not increase with an increase in the number of solder shock cycles.

6.0 CONCLUSIONS

The following conclusions were derived from this study:

- 1) Package cracking may be minimized through proper management of the thermal and

mechanical stresses experienced by the parts during assembly. Three key areas of stress management were identified, namely:

- a) package robustness enhancement;
 - b) minimization of thermal and mechanical stresses inherent to assembly through process and tooling design improvements; and
 - c) elimination of process deviations and/or problems by using effective process controls, monitors, and early detection tests
- 2) Process modelling of each back-end assembly station is an important and practical tool for determining the critical input variables that affect package cracking tendency.

7. ACKNOWLEDGEMENTS

The authors wish to thank the following: Danny Antonio, Jessica Castillo, Carrie Vallespin, Joel Alcantara, and Abet Patupat, who actively participated in the studies and activities that led to the completion of this paper; Jessica Castillo, for allowing us to cite her technical work on early detection tests, Joel Alcantara for sharing his work on Lead Pull analysis, Kieran Harney for the motivation, the Management of Analog Devices Phils., Inc. for their support and permission to publish this work, and Liza Marie, Nimfa and Maribel for the inspirations.

8.0 REFERENCES

1. Higdon, et. al.(1978). *Mechanics of Materials*, John Wiley and Sons, New York, U.S.A., pp 239-482.
2. William Nash (1972). *"Strength of Materials"*, McGraw-Hill Book Company, New York, U.S.A., pp. 80-348.
3. Dr. Manolo Mena (1992). *"Materials Science"*, Analog Devices Phils., Inc.
4. Thomas Moore and Robert McKenna (1993). *"Characterization of Integrated Circuit Packaging Materials"*, Butterworths Heinemann, Reed Publishing Inc., Mass., U.S.A., pp. 61-61.
5. Fukuzawa, et. al. (1988). *"Moisture Resistance Degradation of Plastic LSIs by Reflow Solder Process"*, International Reliability Physics Symposium.
6. John H. Lau (1993). *"Thermal Stress and Strain in Micro-electronic Packaging"*, Van Nostrand Rheinhold, pp. 410-44, New York.
7. John Sauber, et.al. (1994). *"Fracture Properties of Molding Compound Materials for IC Plastic Packaging"*, ECTC Proceedings, 1994, Washington D.C., pp. 164-170.
- 8) Joel Alcantara (1993). *"Lead Pull as Additional Test for Plastic Leadframe Characterization"*, Proceedings of the ADPI Technical Symposium.
- 9) Jessica Castillo (1994). *"Hot Solder Shock Test for 't=0' Monitor"*, ADPI Reliability Eng'g Report, Dec. 20, 1994.

